

## Dynamics of Ultrafast Singlet and Triplet Charge Transfer in Anthraquinone–DNA Conjugates

Frederick D. Lewis,\* Arun K. Thazhathveetil, Tarek A. Zeidan, Josh Vura-Weis, and Michael R. Wasielewski\*

Department of Chemistry and Argonne–Northwestern Solar Energy Research (ANSER) Center, Northwestern University, Evanston, Illinois 60208-3113

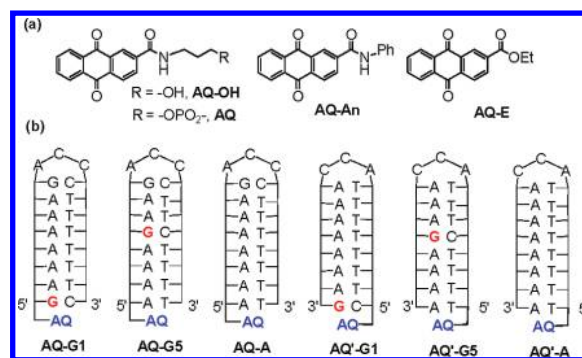
Received October 5, 2009; E-mail: fdl@northwestern.edu; m-wasielewski@northwestern.edu

Anthraquinone (AQ) derivatives have been widely used as phototonucleases in studies of DNA oxidative strand cleavage.<sup>1,2</sup> AQ derivatives undergo rapid intersystem crossing to yield relatively long-lived triplet states that are capable of oxidizing purine nucleobases.<sup>3–5</sup> Charge recombination in the resulting triplet radical ion pairs is spin-forbidden, thus offering an advantage over singlet photooxidants that form singlet radical ion pairs, for which charge recombination is spin-allowed.<sup>6</sup> The formation of long-lived transients assigned to AQ<sup>••</sup> upon inter- and intramolecular quenching by nucleosides in polar organic solvents<sup>7,8</sup> and by duplex DNA in water<sup>3</sup> has been reported. However, the quantum yields for AQ-sensitized strand cleavage are 5% or less.<sup>2,9</sup> Low quantum yields might result from inefficiencies in the generation of the triplet charge-separated state or in the subsequent hole migration and strand cleavage processes. In spite of the extensive use of AQ as a photooxidase in DNA strand cleavage studies, the dynamics of the initial photochemical events (intersystem crossing, singlet and triplet charge transfer, and singlet charge recombination) have not been reported.

We describe here the results of a femtosecond time-resolved transient absorption spectroscopy investigation of the dynamics of charge transfer in DNA hairpin conjugates possessing a tethered AQ end-capping group (Chart 1). Singlet-state electron transfer is faster than intersystem crossing in these conjugates, resulting in more efficient formation of short-lived singlet radical ion pairs than long-lived triplet radical ion pairs.

(*N*-Hydroxypropyl)anthraquinone-2-carboxamide (AQ–OH, Chart 1a) was synthesized by the procedure of Gasper and Schuster<sup>10</sup> and incorporated into the oligonucleotide conjugates shown in Chart 1b and Chart S1 in the Supporting Information by standard phosphoramidite chemistry. The conjugates were characterized by MALDI–TOF mass spectrometry and UV and circular dichroism (CD) spectroscopy (Table S1 and Figure S1 in the Supporting Information). They form hairpin structures in which the AQ is assumed to serve as a capping group<sup>10</sup> attached to either a polypurine or polypyrimidine strand (an AQ or AQ' conjugate, respectively), and the midstrand GACCC or CCA sequences form mini-hairpin loops.<sup>11,12</sup> The hairpin stem regions possess either all A–T base pairs (AQ–A) or a single G–C base pair located at a variable distance from AQ (AQ–G<sub>*n*</sub>, *n* = 1–5). The UV spectra of the conjugates display a weak long-wavelength band at 340 nm assigned to the AQ *n*– $\pi^*$  transition and a stronger band at 260 nm dominated by nucleobase absorption (Figure S1a). The thermal dissociation profile for AQ–G1 in 10 mM sodium phosphate buffer (pH 7.2) with 100 mM NaCl (the standard buffer employed in all of the spectroscopic studies) provided a melting temperature of 61.9 °C (Figure S1b). The CD spectrum of AQ–G1 is characteristic of B-DNA structures possessing multiple A–T base pairs (Figure S1c).<sup>12</sup>

**Chart 1.** (a) Structures of the AQ Derivative AQ–OH, the Hairpin Capping Group AQ, Ester AQ–E, and Dyad AQ–An; (b) Structures of Several AQ- and AQ'-Capped Hairpins



Transient absorption spectra were obtained using a Ti:sapphire laser system having a 200 fs instrument response function and an excitation wavelength of 350 nm.<sup>13</sup> The transient spectra for AQ–OH in aqueous buffer and in methanol (nondeoxygenated) at delay times of 0–1 ns shown in Figure S2 are similar to those recently reported by Harriman and co-workers for the AQ triplet state of the ester AQ–E (Chart 1a).<sup>5</sup> The 450 nm maximum and broad absorption extending beyond 700 nm are formed within the first 1 ps, consistent with the rise time of 0.4 ps reported for formation of the triplet state of AQ–E. The long-lived component of the AQ–OH transient decay is longer than the 6 ns time window of our measurements (Figure S3).

The transient spectra of the conjugates AQ–G5 and AQ–G1 at various delay times are shown in Figure 1, and spectra for the other conjugates are shown in Figure S4 and S5. Bands centered at 406 and 575 nm are formed during the laser pump pulse. The single-wavelength decays of these two bands display both short and long-lived components (Table S2). Within the first few picoseconds, the 406/575 nm band intensity ratio decreases from ca. 2.4 to 1.1 and the 575 nm band undergoes a blue shift to 525 nm. A small decrease in band intensity but no change in band-

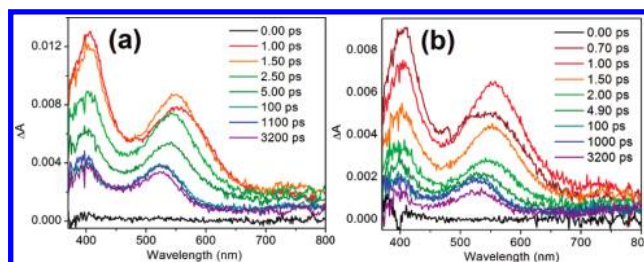


**Figure 1.** Transient absorption spectra for (a) AQ–G5 and (b) AQ–G1 in 10 mM phosphate buffer (pH 7.2, 100 mM NaCl).

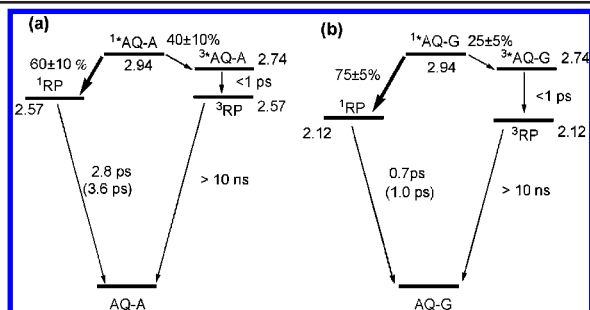


**Figure 2.** Efficiencies of formation and radical-pair decay times of conjugates possessing neighboring (a) A–T and (b) G–C base pairs. Values in parentheses are for the AQ' series. Estimated energies are given in eV (see the Supporting Information).

maximum position occurs during the ensuing 6 ns time window of our measurements. The decay components for **AQ–G1** and **AQ'–G1** are somewhat faster than those for the other conjugates, all of which are similar (Table S2). Thus, the decay times are primarily determined by the identity of the neighboring base pair (G–C or A–T).

The two transient absorption bands observed for all of the conjugates are assigned to  $AQ^{\cdot-}$ . This assignment is consistent with the nanosecond transient spectra reported by Armitage et al.<sup>3</sup> for an AQ derivative intercalated in calf thymus DNA and by Netzel et al.<sup>8</sup> for an AQ–adenine dyad. The blue shift of the longer-wavelength band that occurs during the first few picoseconds is attributed to solvent and nuclear relaxation of  $AQ^{\cdot-}$ .<sup>14</sup> The fast decay of the 406/575 nm band intensity ratio is tentatively attributed to the decay of the  $^3AQ$  transient, whose absorption band (Figure S2) overlaps with the 406 nm band of  $AQ^{\cdot-}$ .

The behavior of the AQ singlet and triplet excited states having neighboring A–T or G–C base pairs is summarized in Figure 2, which is consistent with the kinetic scheme proposed by Schuster and co-workers.<sup>9,15</sup> The rise times for the 525–575 nm bands assigned to  $AQ^{\cdot-}$  are instrument-limited (ca. 200 fs), thus establishing that decay of  $^1AQ$  is complete within this time window. The absence of a resolved 450 nm band for  $^3AQ$  and the fast decay of the 406/525 nm band intensity ratio indicate that triplet radical pair formation also occurs on the subpicosecond time scale (Figure 2). The relative efficiencies of the formation of singlet and triplet radical ion pairs ( $^1RP$  and  $^3RP$ ) can be estimated from the amplitudes for fast and slow decay of the 525–575 nm band. As seen in Figure 2 and Table S2, formation of  $^1RP$  is the major process for most of the conjugates investigated. The preference for  $^1RP$  formation is larger for neighboring G–C versus A–T base pairs and for the AQ' versus the AQ series.

The preferential formation of  $^1RP$  over  $^3RP$  could be the consequence of either competing first-order  $^1AQ$  decay processes (as indicated in Figure 2) or reactions of two kinetically nonequivalent conformations. The single-point attachment of the AQ chromophore does not define its location with respect to the neighboring base pair(s). Both capping and intercalated conformations have been observed for conjugates having a 5'-tethered stilbene or pyrene.<sup>16</sup> Competing first-order reactions would require time constants of  $\leq 0.3$  ps for  $^1RP$  formation ( $\tau_{rp}$ ) and  $\leq 0.5$  ps for intersystem crossing ( $\tau_{isc}$ ) in hairpins having neighboring A–T base pairs. The former value is comparable to the shortest lifetime previously observed for DNA hairpins having linker chromophores that serve as singlet-state electron acceptors.<sup>17</sup> The latter value is consistent with the value of  $\tau_{isc} = 0.4$  ps reported for **AQ–E**.<sup>5</sup>

The  $^1RP$  recombination times ( $\tau_{cr}$ ) shown in Figure 2 are similar to the 2 ps decay time for the dyad $^1(AQ^{\cdot-}-An^{+})$  (Chart 1a).<sup>5</sup> These

values of  $\tau_{cr}$  are much shorter than the value of ca. 1 ns/base pair estimated from the rate constants for hole migration in DNA A-tracts.<sup>18</sup> Thus, ultrafast singlet charge separation–charge recombination results in a substantial reduction in the formation of the long-lived  $^3RP$  intermediates responsible for strand cleavage. The values of  $\tau_{cr}$  are somewhat longer for the AQ' series than for the AQ series. This difference may reflect differences in  $^1RP$  geometries.

In summary, we have found that singlet charge separation is more efficient than intersystem crossing in AQ hairpin conjugates when either A–T or G–C is the neighboring base pair. In fact, the initial yields of long-lived  $^3RP$  are not significantly larger than those for the long-lived singlet charge-separated states observed in our studies of stilbene donor–acceptor capped hairpins.<sup>18</sup> Thus, the expected advantage of using a triplet sensitizer for efficient hole injection in DNA is not fully realized in the AQ–DNA systems we have investigated. The dynamics of the slower events (triplet hole migration, radical-pair intersystem crossing, charge recombination, and reactions of the guanine cation radical) that determine the base-sequence dependence of the AQ-sensitized strand cleavage efficiency remain to be elucidated.

**Acknowledgment.** This work was supported by the Chemical Sciences, Geosciences, and Biosciences Division, Office of Basic Energy Sciences, DOE, under Grants DE-FG02-96ER14604 (F.D.L.) and DE-FG02-99ER14999 (M.R.W.).

**Supporting Information Available:** MALDI-TOF analysis of capped hairpins; UV, fluorescence, and circular dichroism spectra; thermal dissociation profiles; and transient absorption spectra and kinetics. This material is available free of charge via the Internet at <http://pubs.acs.org>.

## References

- (1) (a) Armitage, B. *Chem. Rev.* **1998**, *98*, 1171. (b) Schuster, G. B. *Acc. Chem. Res.* **2000**, *33*, 253. (c) Schuster, G. B.; Landman, U. *Top. Curr. Chem.* **2004**, *236*, 139. (d) Fahlman, R. P.; Sharma, R. D.; Sen, D. *J. Am. Chem. Soc.* **2002**, *124*, 12477. (e) Shao, F. W.; Augustyn, K.; Barton, J. K. *J. Am. Chem. Soc.* **2005**, *127*, 17445. (f) Bergeron, F.; Nair, V. K.; Wagner, J. R. *J. Am. Chem. Soc.* **2006**, *128*, 14798.
- (2) Williams, T. T.; Dohno, C.; Stemp, E. D. A.; Barton, J. K. *J. Am. Chem. Soc.* **2004**, *126*, 8148.
- (3) Armitage, B.; Yu, C. J.; Devadoss, C.; Schuster, G. B. *J. Am. Chem. Soc.* **1994**, *116*, 9847.
- (4) Okamoto, K.; Hasobe, T.; Tkachenko, N. V.; Lemmetyinen, H.; Kamat, P. V.; Fukuzumi, S. *J. Phys. Chem. A* **2005**, *109*, 4662.
- (5) van Ramesdonk, H. J.; Bakker, B. H.; Groeneveld, M. M.; Verhoeven, J. W.; Allen, B. D.; Rostron, J. P.; Harriman, A. *J. Phys. Chem. A* **2006**, *110*, 13145.
- (6) Verhoeven, J. W. *J. Photochem. Photobiol., C* **2006**, *7*, 40.
- (7) Ma, J. H.; Lin, W. Z.; Wang, W. F.; Han, Z. H.; Yao, S. D.; Lin, N. Y. *Radiat. Phys. Chem.* **1999**, *54*, 491.
- (8) Hussein, Y. H. A.; Anderson, N.; Lian, T. T.; Abdou, I. M.; Strekowski, L.; Timoshchuk, V. A.; Vaghefi, M. M.; Netzel, T. L. *J. Phys. Chem. A* **2006**, *110*, 4320.
- (9) Saniil, L.; Schuster, G. B. *J. Am. Chem. Soc.* **2000**, *122*, 11545.
- (10) Gasper, S. M.; Schuster, G. B. *J. Am. Chem. Soc.* **1997**, *119*, 12762.
- (11) Yoshizawa, S.; Kawai, G.; Watanabe, K.; Miura, K.; Hirao, I. *Biochemistry* **1997**, *36*, 4761.
- (12) Lewis, F. D.; Zhang, L.; Liu, X.; Zuo, X.; Tiede, D. M.; Long, H.; Schatz, G. S. *J. Am. Chem. Soc.* **2005**, *127*, 14445.
- (13) Zeidan, T. A.; Carmieli, R.; Kelley, R. F.; Wilson, T. M.; Lewis, F. D.; Wasielewski, M. R. *J. Am. Chem. Soc.* **2008**, *130*, 13945.
- (14) The 50 nm difference in the positions of the band maxima for  $^3AQ$  and both the  $^1RP$  and  $^3RP$  states can be attributed to solvent and nuclear relaxation. Time-dependent density functional theory calculations for  $AQ^{\cdot-}$  at the optimized geometries of the neutral and anion radical display a 50 nm band shift (from 608 to 556 nm).
- (15) Ly, D.; Kan, Y. Z.; Armitage, B.; Schuster, G. B. *J. Am. Chem. Soc.* **1996**, *118*, 8747.
- (16) (a) Tuma, J.; Paulini, R.; Rojas Stutz, J. A.; Richert, C. *Biochemistry* **2004**, *43*, 15680. (b) Siegmund, K.; Daublain, P.; Wang, Q.; Trifonov, A.; Fiebig, T.; Lewis, F. D. *J. Phys. Chem. B* **2009**, *113*, 16276.
- (17) Lewis, F. D.; Kalgutkar, R. S.; Wu, Y.; Liu, X.; Liu, J.; Hayes, R. T.; Wasielewski, M. R. *J. Am. Chem. Soc.* **2000**, *122*, 12346.
- (18) Vura-Weiss, J.; Wasielewski, M. R.; Thazhathveetil, A. K.; Lewis, F. D. *J. Am. Chem. Soc.* **2009**, *131*, 9722.

JA908470D